Eur. J. Mineral.
2002, **14**, 459–469

Sodium and potassium in cordierite – a potential thermometer for melts?

PAULINE THOMPSON*, SIMON L. HARLEY and DAMIAN P. CARRINGTON**

Department of Geology and Geophysics, University of Edinburgh, Kings Buildings, West Mains Road, Edinburgh EH9 3JW, U.K.
** Online News Editor, New Scientist, 151 Wardour St., London W1F 8WE, U.K.
* corresponding author: e-mail: Pauline.Thompson@glg.ed.ac.uk

Abstract: K_2O and Na_2O contents of a low-Be-Li cordierite coexisting with a granitic melt, characterised by a near constant Na/K ratio of 1.39 (in atomic proportions), have been determined as a function of P, T, aH_2O and aCO_2 in the range 3-7 kbar and 800-1000 °C. aH_2O and aCO_2 were calculated for individual experiments using measured H_2O contents of cordierite and melt, and CO_2 contents of cordierite. Na in the cordierite does not vary with P, T aH_2O or aCO_2 within this experimental range. The Na_2O content is within analytical error of the value 0.120 wt% Na_2O in all these experiments and thus does not support previous experimental results that showed more variable Na contents. K in cordierite increases (from 0.03 to 0.18 wt% K_2O) with increasing T and decreasing aH_2O (H_2O content in cordierite and melt) but is not influenced by aCO_2.

The measured variations in K/Na in cordierite (in atoms per formula unit) are systematic with T and aH_2O. The following expression describing the temperature dependence of cordierite-melt K, Na exchange for a melt with a fixed alkali composition of 4.79 wt% K_2O and 4.37 wt% Na_2O can therefore be derived

$$T = -10890\ (\pm\ 3400) / [1n\left(\frac{K}{Na}\right) - 9.539\ (\pm\ 2.850) + 1.303\ (\pm\ 0.427)\sqrt{aH_2O}],$$

where T is in degrees Kelvin. This can be used, with due caution, as a relative or absolute thermometer for approximating the temperature (*e.g.* absolute uncertainty of ±45 °C at the centre of the experimental range studied) at which cordierite and granitic melt last equilibrated. The effect of variations in the melt composition from that used in our experiments may add to the uncertainty in any absolute temperature estimates. However, by comparison with experimentally determined minimum melt compositions, the thermometer is applicable to any melt formed at a water activity of less than 0.5 over the entire pressure range of cordierite-melt stability (1-8 kbar). At higher water activities approaching unity the equation above is only applicable at low pressures. Application of this thermometer requires the availability of high-quality analytical data for H_2O, K and Na in low-Li and -Be cordierite, and its precision is limited at lower temperatures by the difficulties in measuring the low K_2O contents expected in cordierites formed with granitic melts.

Key-words: sodium, potassium, cordierite, granitic melt, thermometer.

Introduction

Among the alkalis, Na, K and Li are minor components of natural cordierites that have often been attributed particular significance because they are sited at or around the "nodes" between the cages along the channels in the room temperature cordierite structure (*e.g.* Kolesov & Geiger, 2000; Armbruster, 1986; Schreyer *et al*., 1979; Kim *et al*., 1984; Wolfsdorff & Schreyer, 1992). They may potentially influence the kinetics and magnitude of volatile uptake (Johannes & Schreyer, 1981). Sodium has commonly been found to occur in natural cordierites, usually in the range of 0-0.5 wt% Na_2O but occasionally up to 1.25 wt% Na_2O (Schreyer *et al*., 1979). In contrast, the potassium content is often very low and commonly ignored either because it lies beneath detection levels or because it is presumed to be a contamination problem from pinitisation. However, Schreyer *et al*. (1990) discovered that potassic cordierites were characteristic minerals in high-temperature, low-pressure environments of the sanidinite facies. Their samples from Blaue Kuppe contained up to 1.71 wt% K_2O. Furthermore, Flood & Shaw (1975) and Clemens & Wall (1984) described cordierites from magmatic environments with 0.08-0.1 wt% K_2O. Most other published cordierites analyses contain negligible quantities of less than 0.03 wt% K_2O.

Cordierite sodium contents from experiments have been observed to decrease with temperature and have been used to develop a preliminary geothermometer (Mirwald, 1986) for rocks that also contain a sodic plagioclase. The sodium contents reported by Mirwald (1986) ranged from approximately 0.08 atoms per formula unit (a.p.f.u) (equivalent to 0.40 wt% Na_2O) at 650 °C to 0.02 a.p.f.u at 850 °C. This

DOI: 10.1127/0935-1221/2002/0014-0459
0935-1221/02/0014-0459 $ 4.95

Na-in-cordierite thermometer was found to give reasonable (*i.e.* geologically sensible) results when tested by Kalt *et al*. (1998) for contact metamorphosed rocks from the island of Kos. Subsequent experimental data (Knop & Mirwald, 2000) confirmed that the sodium content in magnesian cordierite is inversely related to temperature but also decreases significantly if CO_2 is present in the experiments. They observed that the cordierite Na content significantly increased above the albite-cordierite eutectic temperature (680 °C) but still decreased with increasing temperature over the range 700-850 °C in the presence of a partial melt.

We have conducted two suites of experiments on a natural cordierite at 3-7 kbar and 800-1000 °C and at a variety of fluid compositions. One suite of experiments contained only H_2O as a volatile species and ranged from fluid-saturated to -undersaturated with H_2O activities down to 0.12. The other suite was all fluid-saturated with an H_2O-CO_2 fluid that caused the H_2O activity to vary between 1 and 0.16. The aim these two sets of experiments was primarily to establish activity models for H_2O and CO_2 and the relationship between fluids, melts and cordierites at conditions appropriate to granulite metamorphism. These activity models have been reported in Carrington & Harley (1996), Harley & Carrington (2001), Thompson *et al*. (2001) and Thompson & Harley (in prep.). Our two suites of experiments thus provide a large dataset with known volatile contents, pressure and temperature conditions that we can use to compare with the previous studies of cordierite Na contents and provide new data on variations in K.

Experimental and analytical techniques

Experiments were performed at 3-7 kbar and 800-1000 °C in an internally heated gas apparatus that has pressure and temperature uncertainties of ±0.2 kbar and ±5 °C respectively (Carrington & Harley, 1995). The experimental charges each initially contained an evacuated, natural, orthorhombic cordierite BB3a (grain size 125-250 μm diameter), a gel of granitic melt composition and a variable composition and proportion of fluid. The cordierite had been evacuated of all volatiles prior to the experiment by prolonged step-heating in a high vacuum at temperatures of up to 1200 °C (Thompson *et al*., 2001). The compositions of the evacuated cordierite, BB3a, and melt starting materials are given in Table 1. The cordierite was from restitic veins in the migmatitic Brattstrand Bluffs granulites of Prydz Bay, Antarctica (Fitzsimons, 1996). This cordierite, BB3a, contains negligible Li (16 ppm) and low Be (30-100 ppm) as measured by secondary ion mass spectroscopy (SIMS). This Be content is similar to the Be-free cordierites of Schreyer *et al*. (1979). The H_2O and CO_2 contents of this cordierite, once evacuated, were lower than the detection limits of SIMS (H_2O < 0.16 wt%, CO_2 <0.08 wt%). The ratio of cordierite to melt was always approximately 5:14, both before and after the experiment. Occasional minor alteration of the cordierite occurred to form spinel but on such a small scale that it would not affect the proportions of volatile and alkali bearing phases.

Table 1. Compositions of the evacuated cordierite and melt gel starting materials.

	BB3a	Melt gel
SiO_2	48.12	73.57
Al_2O_3	33.02	15.05
FeO	8.61	1.82
MgO	8.57	0.40
K_2O	0.03	4.79
Na_2O	0.05	4.37
Total	98.42	100.00
X_{Mg}	0.64	0.28

Note: Melt data has been normalised

The final volatile contents of cordierite and melt in the experiments were obtained by the introduction of varied quantities of H_2O in the H_2O-only system, or a range of fluid compositions in the H_2O-CO_2 fluid-saturated experiments. The fluid-saturated experiments are indicated in Table 2 and full details of experimental charges and runs are given in Harley and Carrington (2001) for the H_2O-only experiments and Thompson *et al.* (2001), Thompson & Harley (in prep.) for the H_2O-CO_2 experiments. All experiments were run for between 137 and 524 hours. Time studies in both the H_2O-only system (Harley & Carrington, 2001) and the H_2O-CO_2 system (Thompson *et al*., 2001) have shown that these run durations are sufficient to reach equilibrium in the other channel components, H_2O and CO_2. Equilibrium in the channel alkalis is harder to establish due to the difficulties in measuring alkalis in the melt phase. Although we have conducted experiments of different duration, keeping all other variables constant is difficult and thus we cannot prove that these alkali contents are equilibrium values. Nevertheless, the consistency in results between H_2O-only and H_2O-CO_2 experiments, together with the overall coherency in the trends defined by the Na_2O and K_2O contents when plotted against the other experimental variables, give us confidence that the alkali contents approach equilibrium.

SIMS was used to determine the H_2O and CO_2 contents of the cordierites. All other oxides were measured with a wavelength-dispersive electron microprobe (EMP) in Edinburgh at 20 kV and a low beam current of 10 nA. Care was taken to avoid volatilisation of the sodium in particular by minimising the dwell time on each spot prior to each analysis and by analysing the sodium and potassium first. A rastered beam of 10 μm diameter was also used to minimise volatilisation although there was no noticeable difference between a rastered beam and a spot when analysing cordierites. The detection limits were approximately 0.03 wt% for Na_2O and 0.04 for K_2O. The melts were analysed by wavelength-dispersive electron microprobe (EMP) complemented by energy-dispersive scanning electron microscopy (SEM) using a cold stage (Manchester). The melts showed very little change in composition throughout the duration of the experiment (Thompson & Harley, in prep.). For full details of all experimental techniques and analytical conditions see Carrington & Harley (1996), Harley & Carrington (2001) and Thompson *et al*. (2001).

Table 2. Compositions of cordierites. H_2O and CO_2 analyses are obtained from SIMS and Na_2O, K_2O and X_{Mg} from the electron microprobe. Standard deviations are given on populations of 8-10 analyses for the SIMS data, 8-15 analyses for the electron probe data for the H_2O-CO_2 experiments and 4-8 analyses for the H_2O experiments. For an approximate conversion to atoms or molecules per formula unit for this cordierite composition the weight percentages must be multiplied by 0.338 for H_2O, 0.138 for CO_2, 0.20 for Na and 0.133 for K. * = fluid-saturated experiments.

	P (kbar)	T (°C)	wt% H_2O	σ	aH_2O	σ	wt% CO_2	σ	X_{Mg}	σ	wt% Na_2O	σ	wt% K_2O	σ
Starting material														
BB3a			0.00				0.00		0.64		0.05		0.03	
H_2O experiments														
MP11b	5	900	1.69	0.06	0.888	0.045	0.00		0.627	0.001	0.141	0.031	0.060	0.016
MP8	5	900	1.49	0.08	0.676	0.051	0.00		0.633	0.002	0.130	0.006	0.067	0.010
MP13b*	5	900	1.70	0.05	0.900	0.037	0.00		0.639	0.006	0.125	0.010	0.044	0.012
MP2	5	900	0.45	0.02	0.120	0.008	0.00		0.627	0.002	0.090	0.008	0.138	0.021
MP3	5	900	0.56	0.05	0.156	0.020	0.00		0.632	0.003	0.088	0.023	0.111	0.004
MP5	5	900	0.77	0.05	0.234	0.022	0.00		0.630	0.004	0.120	0.004	0.120	0.003
MP6	5	900	1.30	0.05	0.522	0.028	0.00		0.641	0.014	0.151	0.011	0.109	0.035
MP7	5	900	1.54	0.05	0.723	0.033	0.00		0.627	0.005	0.126	0.006	0.069	0.017
C4-1	5	900	1.11	0.03	0.400	0.015	0.00		0.634	0.002	0.089	0.033	0.076	0.008
C4-A	5	900	1.29	0.03	0.515	0.017	0.00		0.634	0.051	0.119	0.048	0.065	0.042
C4-B	5	900	1.38	0.06	0.583	0.036	0.00		0.629	0.000	0.111	0.000	0.073	0.000
C4-C	5	900	0.85	0.05	0.269	0.022	0.00		0.632	0.001	0.112	0.001	0.107	0.001
DG4	5	900	1.28	0.07	0.508	0.039	0.00		0.626	0.001	0.120	0.001	0.120	0.001
C6-1*	5	800	1.79	0.07	0.824	0.046	0.00		0.634	0.011	0.116	0.019	0.022	0.018
C6-3	5	800	1.11	0.03	0.323	0.012	0.00		0.625	0.001	0.139	0.002	0.056	0.027
C6-5	5	800	1.54	0.05	0.584	0.027	0.00		0.629	0.008	0.140	0.030	0.035	0.010
C6-6	5	800	1.21	0.05	0.373	0.022	0.00		0.624	0.004	0.128	0.028	0.045	0.014
C7-2	5	800	1.63	0.09	0.660	0.052	0.00		0.639	0.009	0.142	0.040	0.047	0.001
C5-3	5	1000	0.88	0.04	0.346	0.022	0.00		0.636	0.015	0.091	0.012	0.128	0.032
C5-4	5	1000	0.36	0.01	0.113	0.004	0.00		0.628	0.007	0.104	0.012	0.170	0.028
C11-1*	3	800	1.44	0.03	1.027	0.030	0.00		0.629	0.004	0.142	0.029	0.039	0.015
C8-1	3	900	1.11	0.06	0.812	0.062	0.00		0.627	0.005	0.109	0.006	0.084	0.005
C8-2	3	900	0.85	0.05	0.545	0.045	0.00		0.626	0.005	0.138	0.008	0.061	0.014
C8-4	3	900	1.17	0.05	0.885	0.053	0.00		0.652	0.020	0.141	0.039	0.060	0.041
C8-5	3	900	0.71	0.04	0.427	0.034	0.00		0.628	0.002	0.139	0.000	0.107	0.035
C14-2	7	900	1.91	0.14	0.726	0.075	0.00		0.628	0.003	0.093	0.014	0.086	0.010
H_2O-CO_2 experiments														
13-1*	5	900	1.69	0.07	0.888	0.049	0.26	0.05	0.641	0.023	0.132	0.071	0.073	0.007
13-5*	5	900	0.89	0.04	0.285	0.018	0.80	0.06	0.639	0.003	0.125	0.031	0.120	0.007
13-4*	5	900	1.33	0.07	0.546	0.039	0.64	0.07	0.627	0.005	0.123	0.017	0.089	0.008
13-2*	5	900	1.73	0.08	0.936	0.061	0.29	0.01	0.635	0.003	0.128	0.006	0.053	0.011
13-3*	5	900	1.59	0.07	0.772	0.048	0.44	0.04	0.636	0.003	0.131	0.012	0.068	0.007
27-2*	3	900	1.18	0.07	0.897	0.080	0.22	0.04	0.634	0.003	0.109	0.009	0.084	0.007
27-5*	3	900	0.77	0.05	0.478	0.047	0.35	0.04	0.634	0.002	0.101	0.013	0.115	0.007
27-3*	3	900	1.25	0.10	0.990	0.109	0.25	0.04	0.634	0.002	0.092	0.019	0.079	0.008
27-4*	3	900	0.85	0.06	0.544	0.053	0.33	0.06	0.636	0.005	0.109	0.010	0.103	0.003
20-3*	5	900	1.29	0.12	0.513	0.070	0.63	0.07	0.635	0.006	0.111	0.019	0.106	0.006
19-4*	5	900	0.57	0.03	0.158	0.010	1.01	0.14	0.631	0.003	0.075	0.010	0.125	0.006
33-1*	5	800	1.65	0.13	0.674	0.072	0.18	0.03	0.635	0.003	0.162	0.017	0.049	0.005
33-5*	5	800	1.24	0.08	0.389	0.035	0.86	0.05	0.635	0.003	0.130	0.011	0.059	0.008
29-2*	7	900	1.77	0.19	0.593	0.092	0.78	0.13	0.634	0.006	0.127	0.016	0.053	0.005
29-3*	7	900	1.26	0.15	0.294	0.049	1.01	0.06	0.638	0.002	0.151	0.011	0.084	0.003
29-5*	7	900	0.92	0.01	0.178	0.002	1.46	0.15	0.635	0.002	0.124	0.006	0.108	0.010
29-4*	7	900	1.07	0.06	0.225	0.018	1.35	0.05	0.624	0.004	0.132	0.017	0.105	0.006
34-3*	5	1000	1.56	0.12	0.909	0.096	0.53	0.03	0.651	0.015	0.094	0.011	0.102	0.007
42-7*	3	1000	0.49	0.02	0.298	0.020	0.34	0.01	0.638	0.012	0.096	0.056	0.178	0.009

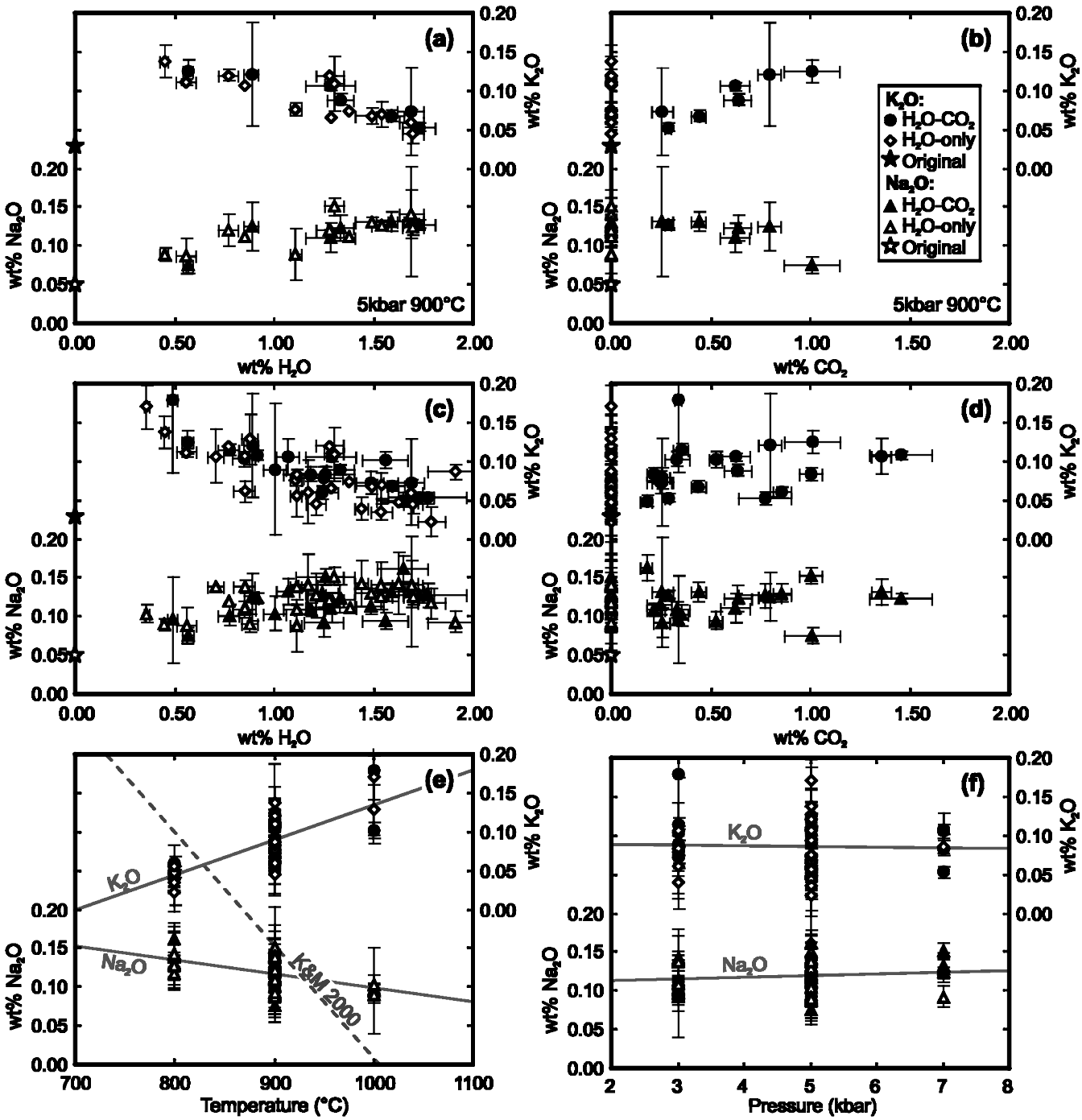

Fig. 1. Variation of weight percentages of Na_2O and K_2O in cordierites with pressure, temperature and weight percentages of H_2O and CO_2. (a) and (b) show data from 5 kbar, 900 °C experiments, (c), (d), (e) and (f) are from all pressures and temperatures studied. For ease of reading the Na_2O and K_2O values have been plotted on the same scales but displaced from one another with Na_2O relating to the y-axis scales on the left and K_2O to the y-axis scales on the right of each diagram. For key to symbols see inset in (b). The dashed line in (e) is the variation of Na_2O with temperature observed by Knop & Mirwald in the presence of albite and at $aH_2O = 1$ (pers. comm., 2000). Lines labelled Na_2O and K_2O are best-fit lines through our data.

Analytical results

The elements that make up the framework of the cordierite did not change significantly in most experiments. Analyses of the mean cordierite channel occupancy for each experiment are shown in Table 2 where, at room temperature, H_2O and CO_2 are likely to be held within the "channel" cages and Na in the "channel" necks (*e.g.* Schreyer, 1985). At room temperature K is located just above and below the six-fold rings in synthetic K-substituted hexagonal cordierite (Kim

et al., 1984). However, Aines & Rossman (1984) showed that, although H_2O is ordered at room temperature and pressure, at high temperatures its position and orientation are more disordered. This loss of order may also be mirrored by the alkalis at high temperatures.

Fig. 1 shows six graphs of the Na_2O and K_2O variation in cordierite BB3a with H_2O content, CO_2 content, pressure and temperature. For clarity the results from 5 kbar and 900 °C are shown separately. Table 1 and the first row of Table 2 give the initial composition of the cordierite starting material that contained 0.05 wt% Na_2O (370 ppm Na) and 0.03 wt% K_2O (250 ppm K) measured on the electron probe. Sodium measured with SIMS was found to give an identical value, within error, of 440 ppm (0.06 wt% Na_2O). Almost all the post-run compositions have an increased Na and K content supplied by the Na- and K-rich granitic melt. On these six graphs both the H_2O-only and the H_2O-CO_2 experiments have been plotted. There is no appreciable difference between the two sets of data.

Variation in cordierite Na and K contents

We measured compositional profiles across cordierite grains to examine whether Na_2O or K_2O changed in close proximity to the melt and found very little systematic variation across any given grain. In a few experiments at higher pressure and more water-rich conditions, cordierite displays more magnesian rims (X_{Mg} of up to 0.75, not included in Table 2) up to 10 μm wide (Harley & Carrington, 2001). Despite this evidence for Fe and Mg disequilibrium, Na and K do not appear to increase in close proximity to the melts. The data we present here in Fig. 1a to f for the H_2O-CO_2 data are mean values taken from throughout these cordierites. In the H_2O-CO_2 experiments occasional cordierite analyses were high in alkalis, but no systematic zoning was observable. Care was taken not to collect analyses from 'free' surfaces of cordierite that were not enclosed by melt, in order to limit the possibility of any influence of quench-related fluid-cordierite exchange on the alkali contents measured.

In the water-rich experiments of the H_2O-only system cordierite is observed to resorb or react along the boundaries and cracks in the cordierite grains to form minor amounts of spinel and a melt that contains a larger proportion of Na and K. This is considered to reflect localised incongruent melting of the cordierite (Harley & Carrington, 2001). It can be difficult to identify the edge of the cordierite-melt interface in these cases, even using back scattered electron imaging. Hence, in these water-rich experiments rastered cordierite rim analyses may be partly contaminated by melt, leading to higher measured values for Na_2O and K_2O. Analyses within 15 μm of the boundaries were therefore omitted when calculating the mean cordierite compositions in the H_2O-only experiments.

Sodium contents

Na_2O varies little within the errors of measurement. There may be a very slight increase in Na_2O with H_2O content, as seen in the 5 kbar, 900 °C data (Fig. 1a). An apparent inverse variation of Na_2O with CO_2 content at 5 kbar, 900 °C (Fig. 1b) relies strongly on the most CO_2-rich point and is not supported by the data as a whole (Fig. 1d). Na_2O appears to decrease very slightly with T (Fig. 1e), by approximately 1.8×10^{-4} wt% Na_2O/ °C (= 3.5×10^{-5} apfu/ °C) but this effect is very small and may not be real. There is no apparent variation with pressure (Fig. 1f). Such simplified two-dimensional plots may mask any covariation between these variables. If there was a slight negative dependence of Na_2O on temperature one might expect it to show a small positive correlation with water content, as water content in cordierite is inversely related to temperature (Harley & Carrington, 2001). However, diagrammatic evaluation of these variables did not demonstrate any such relationship. Thus we analysed the data by stepwise regression using the programme Minitab 12 (see reference list for source), with an appropriate F-statistic for the inclusion or exclusion of a variable set at 4.0. This statistical approach demonstrated that there were no significant predictors for wt% Na_2O amongst all of the variables tested (P, T, wt% H_2O, wt% CO_2, wt% SiO_2, wt% Al_2O_3, wt% FeO, wt% MgO). A slight negative correlation with wt% K_2O was calculated by this procedure but any correlations with temperature or water content were not significant, confirming the results of the simple diagrammatic approach.

Potassium contents

K_2O generally varies more than Na_2O across the range of experimental conditions. K_2O decreases with increasing H_2O content of the cordierite in both the 5 kbar, 900 °C experiments (Fig. 1a) and the data from all P-T conditions studied (Fig. 1c). As temperature increases K_2O in cordierite increases by approximately 4.5×10^{-4} wt% K_2O/ °C (= 6.0×10^{-5} a.p.f.u./ °C), some -2.5 times the Na_2O effect in wt% terms (or -1.7x in a.p.f.u. terms). Stepwise regression (Minitab 12, see reference list for source) on all the raw data (*i.e.* P, T, wt% H_2O, wt% CO_2, wt% SiO_2, wt% Al_2O_3, wt% FeO, wt% MgO, wt% Na_2O) confirms that the wt% K_2O is significantly dependent on both the temperature and wt% H_2O. Stepwise regression also demonstrates that CO_2 and pressure have little impact on wt% K_2O, as can also be seen from the plots of Figures 1b, 1d and 1f.

Thermometer

From the results described above a provisional thermometer can be devised for cordierites that have been in contact with granitic melts of a similar composition to the one we have studied here. This thermometer can either be constructed using an empirical fit to the raw data, or transformed so that the coefficients obtained have some thermodynamic significance. Although the variations in K and Na are not of equivalent magnitude, to a first approximation they may be described by an alkali exchange reaction between the melt and the cordierite,

Na-crd + K-melt = K-crd + Na-melt. (1)

The exchange may be more complex than this, in that it may involve a number of structural sites and other cations. The data presented here do not warrant the development of a more complex model, as can be shown by consideration of the analytical errors. The total cations per cordierite formula unit is consistently higher than 11 in these experiments. This excess is explicable by the alkalis lying in channel sites and not in the framework of the cordierite, in agreement with previous interpretations (*e.g.* Schreyer, 1985). Accordingly, we have examined our data for the coupled substitution Al + alkali → □ + Si, following the methods of Schreyer *et al.* (1990) and Wolfsdorff & Schreyer (1992). If the substitution mechanism is Al + alkali → □ + Si, we would expect our most alkali-rich samples to exhibit a 0.05 a.p.f.u increase in Al (from 4 a.p.f.u.) and decrease in Si (from 5 a.p.f.u.) relative to alkali-free cordierite. However, the maximum *difference* in Al or Si between our most alkali-rich and alkali-poor cordierites expected from the observed variations in alkalis should only be 0.02 a.p.f.u. (*e.g.* 4.03 to 4.05 a.p.f.u. in the case of Al). Errors in the measurement accuracy of Si and Al make such small differences indistinguishable with the analytical data obtained here. This does not negate the possibility of the substitution mechanism proposed by Schreyer *et al.* (1990) controlling the alkali contents of our cordierites, but likewise does not allow us to define the substitution with any degree of confidence.

The equilibrium constant for reaction (1) will be related to the activities of each phase by

$$K_{eq} = \left(\frac{a_K^{crd}}{a_{Na}^{crd}}\right) \Big/ \left(\frac{a_{KFMAS}^{melt}}{a_{NaFMAS}^{melt}}\right) \tag{2}$$

The potassium and sodium components of the melt exhibit some non-ideal mixing in the presence of water. This is highlighted by the difference in water solubilities in albite and orthoclase melts of 11.6 and 10.4 wt% H_2O respectively at 5 kbar and 1100 °C (Behrens, 1995). Currently there is little evidence of any significant non-ideal mixing in the cordierite channel sites and so as a first approximation we have assumed ideal behaviour with an activity coefficient of unity. Thus the equilibrium constant may be expressed as

$$K_{eq} = \left(\frac{X_K^{crd}}{X_{Na}^{crd}}\right) \Big/ \left(\frac{\gamma_{KFMAS}^{melt} X_{KFMAS}^{melt}}{\gamma_{NaFMAS}^{melt} X_{NaFMAS}^{melt}}\right) \tag{3}$$

where X and γ are the mole fractions and activity coefficients respectively for each component. Expansion and simplification of (3) leads to the relation

$$K_{eq} = \left(\frac{K}{Na}\right)^{crd} \Big/ \left[\left(\frac{K}{Na}\right)^{melt} \cdot \left(\frac{\gamma_K}{\gamma_{Na}}\right)^{melt}\right] \tag{4}$$

where K and Na are the number of atoms per formula unit. Since in these experiments there is a large reservoir of Na and K in the melt and the cordierite only takes a very small proportion of Na and K into its structure the Na/K ratio for the melt should remain close to constant with an initial value for these experiments of $(Na/K)^{melt} = 1.39$ (calculated from Carrington & Harley, 1996). Our best measurements of alkalis in these melts indicate that they do indeed change very little during the experiment with the $(Na/K)^{melt}$ ratio lying between 1.61 and 1.39 (Thompson & Harley, in prep.). Hence equation (4) becomes

$$K_{eq} = 1.39\left(\frac{K}{Na}\right)^{crd} \Big/ \left(\frac{\gamma_K}{\gamma_{Na}}\right)^{melt} \tag{5}$$

Taking the natural log of equation (5) gives

$$\ln K_{eq} = \ln\left(\frac{K}{Na}\right)^{crd} + \ln 1.39 - \ln\left(\frac{\gamma_K}{\gamma_{Na}}\right)^{melt} \tag{6}$$

We have thus separated $\ln K_{eq}$ into ideal and non-ideal terms. The ideal term is easily calculated for each of our data points but the non-ideal term cannot be evaluated. It is, however, useful to consider what form the non-ideal term may take so that we may devise a thermometer including parameters that more closely approximate expected thermodynamic functions.

If we assume a ternary symmetric regular solution model for the mixing between Na, K and H_2O in the melt (*e.g.* Wood & Fraser, 1977) the activity coefficients can be expressed as

$$\begin{aligned} RT\ln\gamma_K^{melt} &= \left(X_{Na}^{melt}\right)^2 W_{KNa}^{melt} + \left(X_{H_2O}^{melt}\right)^2 W_{KH_2O}^{melt} \\ &+ X_{Na}^{melt} X_{H_2O}^{melt}\left[W_{KNa}^{melt} + W_{KH_2O}^{melt} - W_{NaH_2O}^{melt}\right] \end{aligned} \tag{7}$$

and

$$\begin{aligned} RT\ln\gamma_{Na}^{melt} &= \left(X_K^{melt}\right)^2 W_{KNa}^{melt} + \left(X_{H_2O}^{melt}\right)^2 W_{NaH_2O}^{melt} \\ &+ X_K^{melt} X_{H_2O}^{melt}\left[W_{KNa}^{melt} + W_{NaH_2O}^{melt} - W_{KH_2O}^{melt}\right] \end{aligned} \tag{8}$$

where X terms are again mole fractions of components and the W terms are interaction parameters between the different components in the melt. These interaction parameters are dependent upon temperature but their values are poorly known (Holland & Powell, 1998) or unknown.

A more useful expression in line with equation (6) can be derived from

$$RT\ln\left(\frac{\gamma_K}{\gamma_{Na}}\right)^{melt} = RT\ln\gamma_K^{melt} - RT\ln\gamma_{Na}^{melt}. \tag{9}$$

By substituting equations (7) and (8) into (9) we obtain

$$\begin{aligned} RT\ln\left(\frac{\gamma_K}{\gamma_{Na}}\right)^{melt} &= W_{KNa}^{melt}\left(X_{Na}^{melt} - X_K^{melt}\right)\left(X_{Na}^{melt} + X_K^{melt}\right) \\ &+ \left(X_{H_2O}^{melt}\right)^2\left(W_{KH_2O}^{melt} - W_{NaH_2O}^{melt}\right) + X_{H_2O}^{melt}\left(X_{Na}^{melt} - X_K^{melt}\right)W_{KNa}^{melt} \\ &+ X_{H_2O}^{melt}\left(X_{Na}^{melt} + X_K^{melt}\right)W_{KH_2O}^{melt} - X_{H_2O}^{melt}\left(X_{Na}^{melt} + X_K^{melt}\right)W_{NaH_2O}^{melt}. \end{aligned} \tag{10}$$

Rearranging equation (10) gives

$$\begin{aligned} RT\ln\left(\frac{\gamma_K}{\gamma_{Na}}\right)^{melt} &= \left(X_{Na}^{melt} + X_K^{melt}\right)\left[W_{KNa}^{melt}\left(X_{Na}^{melt} - X_K^{melt}\right) + X_{H_2O}^{melt}\left(W_{KH_2O}^{melt} - W_{NaH_2O}^{melt}\right)\right] \\ &+ \left(X_{H_2O}^{melt}\right)^2\left(W_{KH_2O}^{melt} - W_{KNa}^{melt}\right) + X_{H_2O}^{melt}\left(X_{Na}^{melt} - X_K^{melt}\right)W_{KNa}^{melt} \\ &= X_{H_2O}^{melt}\left(W_{KH_2O}^{melt} - W_{KNa}^{melt}\right)\left[X_K^{melt} + X_{Na}^{melt} + X_{H_2O}^{melt}\right] \\ &+ W_{KNa}^{melt}\left(X_{Na}^{melt} - X_K^{melt}\right)\left[X_K^{melt} + X_{Na}^{melt} + X_{H_2O}^{melt}\right]. \end{aligned} \tag{11}$$

As $[X_K^{melt} + X_{Na}^{melt} + X_{H_2O}^{melt}] = 1$ we can simplify this expression to

$$RT \ln\left(\frac{\gamma_K}{\gamma_{Na}}\right)^{melt} = X^{melt}_{H_2O}\left(W^{melt}_{KH_2O} - W^{melt}_{KNa}\right) + W^{melt}_{KNa}\left(X^{melt}_{Na} - X^{melt}_{K}\right). \quad (12)$$

Although we do not know the three interaction parameters in this equation or their temperature dependence we do know that the mole fractions of Na and K are fairly constant and of similar magnitude. In the starting material the difference between the mole fractions of Na and K in the melt ($X^{melt}_{Na} + X^{melt}_{K}$) is only 0.04, so that the compositional function in the second term in equation (12) is much smaller than the mole fraction of water term *i.e.*

$$X^{melt}_{H_2O}\left(W^{melt}_{KH_2O} - W^{melt}_{KNa}\right) >> W^{melt}_{KNa}\left(X^{melt}_{Na} - X^{melt}_{K}\right)$$

$$>> 0.04 W^{melt}_{KNa}.$$

This implies that $RT \ln(\gamma_K/\gamma_{Na})^{melt}$ is approximately equal to $X^{melt}_{H_2O}$ $(W^{melt}_{KH_2O} - W^{melt}_{KNa}]$. The macroscopic H_2O solubility in relevant granitic melts is approximated by the Burnham model (Burnham & Nekvasil, 1986), so that

$$X^{melt}_{H_2O} = \sqrt{\frac{a_{H_2O}}{k_w}}, \quad (13)$$

where the proportionality term k_w can be evaluated at the P-T condition of the experiments using the approach of Harley & Carrington (2001). The value of k_w ranges from 3.65 at 3 kbar, 800 °C to 2.07 at 7 kbar, 1000 °C. Combining (13) with the approximated version of (12), it follows that $RT \ln(\gamma_K/\gamma_{Na})^{melt}$ is approximately proportional to $\sqrt{aH_2O}$.

If we consider the standard thermodynamic formulation (*e.g.* Spear, 1993)

$$-\ln K_{eq} = \frac{\Delta H(P,T)}{RT} - \frac{\Delta S(P,T)}{R} \quad (14)$$

from (6) and (12) we can write the relationship

$$-\frac{\Delta H(P,T)}{RT} + \frac{\Delta S(P,T)}{R} = \ln\left(\frac{K}{Na}\right)^{crd} + \ln 1.39 - \ln\left(\frac{\gamma_K}{\gamma_{Na}}\right)^{melt}$$
$$= \ln\left(\frac{K}{Na}\right)^{crd} + \ln 1.39 - \frac{\left(W^{melt}_{KH_2O} - W^{melt}_{KNa}\right)}{RT}\frac{\sqrt{aH_2O}}{\sqrt{k_w}} + \frac{0.04}{RT} W^{melt}_{KNa}. \quad (15)$$

We can resolve this expression into the form of a plane $y = A + Bx + Cz$

$$\ln\left(\frac{K}{Na}\right)^{crd} = A + \frac{B}{T} + C\sqrt{aH_2O}, \quad (16)$$

where

$$A = \frac{\Delta S(P,T)}{R} - \ln 1.39,$$

$$B = -\frac{\Delta H(P,T)}{R} - \frac{0.04}{R} W^{melt}_{KNa},$$

$$C = \frac{\left(W^{melt}_{KH_2O} - W^{melt}_{KNa}\right)}{RT\sqrt{k_w}}.$$

(16) is the equation of a plane with axes $\ln(K/Na)^{crd}$, 1/T and $\sqrt{aH_2O}$, where K and Na are in atoms per formula unit and T is in Kelvin. The value of $\ln(K/Na)^{crd}$ in atoms per formula unit can be simply calculated for any cordierite as equivalent to $\ln(wt\%\ K_2O/wt\%\ Na_2O)^{crd} + \ln(62/94)$.

In order to fit a plane through our data we need to calculate the water activity from the water content of the cordierite. This has been done using the model of Harley & Carrington (2001) for water incorporation in cordierite and the values are shown in Table 2. When fitting the plane we could have taken the temperature term out of the C coefficient. However, from our data we can not distinguish a difference in the slope of the activity term at each different temperature and thus for simplicity and to retain independent axes we have fitted the equation as shown above. Thus the equivalent coefficient for a $\sqrt{aH_2O}$ term would be simply our C values divided by the mean temperature (1173 K) of our experiments.

Planar regression is a complex problem as there are errors in all three parameters for each point. We used a York fitting programme (Ludwig, 1992) that is commonly used in geochronology. The programme follows the method of York (1967, 1969) which permits least squares regression in three dimensions with error bars in the *x*, *y* and *z* directions. Thus a plane was fitted to give values of the coefficients A, B and C, their standard deviations and the correlations between A, B and C (Table 3).

The parameters A and B can be converted into approximate values for entropy (ΔS) and enthalpy (ΔH) of the exchange reaction (1) at the average T of the experiments (900 °C). This yields $\Delta S \approx 82$ $JK^{-1}mol$, and $\Delta H \approx 90.5$ $kJmol^{-1}$ to ≈ 89.5 $kJmol^{-1}$ depending upon the magnitude of the melt interaction parameter, W_{KNa} ($0 \leq W_{KNa} \leq 22$ $kJmol^{-1}$, given that there is no unmixing of the melt into K- and Na-rich compositions at $T \leq 1300$ K). Thus, the enthalpy of exchange of K for Na in cordierite is strongly endothermic, and the entropy change for this exchange is of a similar magnitude (but less than) the entropies associated with the liberation of H_2O or CO_2 from cordierite (Harley *et al.*, 2001).

To use this as a geothermometer, equation (16) is rewritten as

$$T = B\Big/\left[\ln\left(\frac{K}{Na}\right)^{crd} - A - C\sqrt{aH_2O}\right]. \quad (17)$$

Unlike a standard regression that only allows for *y*-residuals, the York fitting programme (Ludwig, 1992) does give equivalent coefficients for an identical plane whichever axes are chosen as the input. Thus rearranging the equation and propagating the errors in a standard manner is reasonable in order to obtain the statistical error in the fit of the plane (see Appendix). Fig. 2a shows a projection of our data

Table 3. Coefficients, 1σ errors and correlation coefficients for the terms of equation (14) when K and Na are given in atoms per formula unit and T in Kelvin.

Coefficient	Value	1σ error	Correlation coefficient	Value
A	9.539	2.850	ρ_{AB}	-0.9952
B	-10890	3400	ρ_{BC}	-0.2060
C	-1.303	0.427	ρ_{AC}	0.1121

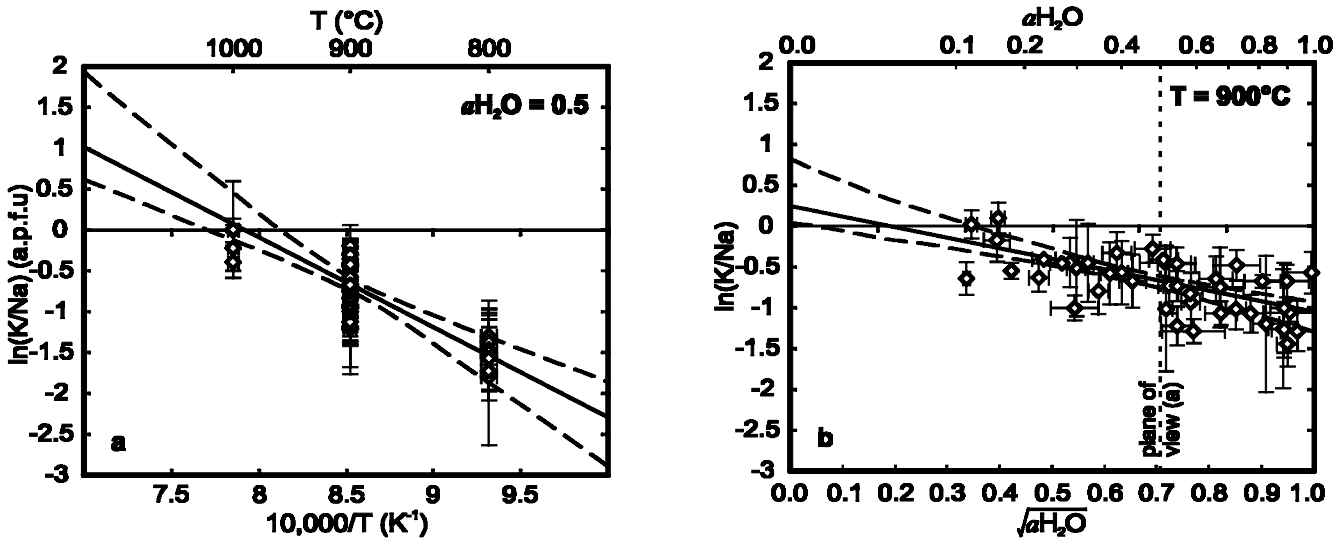

Fig. 2.a) A plot of cordierite ln(K/Na) against 10^4/T data used for fitting the plane (equation 16), projected along the plane to $aH_2O = 0.5$. The solid line is our modelled plane and the dashed lines are the propagated 1σ errors in the fit of the plane at a water activity of 0.5. b) An equivalent projection along the fitted plane to show the dependence of ln(K/Na) with aH_2O.

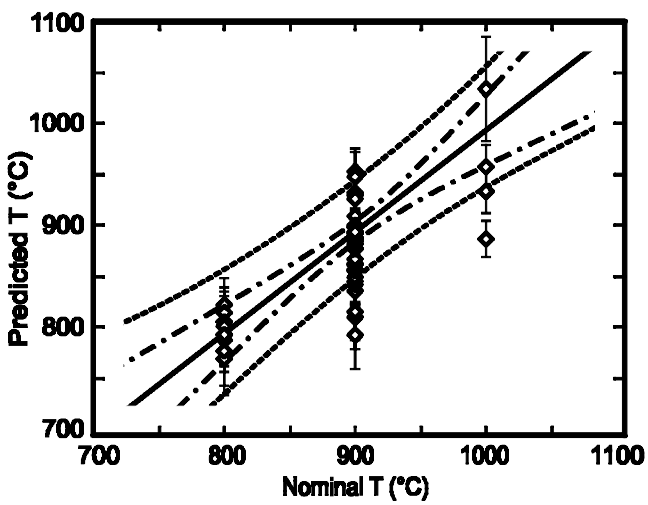

Fig. 3. The predicted temperature for each of the original data points has been calculated using equation (18) and plotted against the true temperature of the experiment (Nominal T). The predicted T for any nominal T is given by the solid line. The two dot-dash lines are the 1σ envelope in the fit of the original plane i.e. the precision of the thermometer at $aH_2O = 0.5$. The dashed lines are an approximate 1σ envelope for the accuracy of the thermometer (see text for discussion). When an absolute temperature is required the larger errors must be used but for a temperature difference the precision (plane fitting error) is sufficient.

along the plane onto the $\ln(K/Na)^{crd}$ *vs* 1/T plane at aH_2O = 0.5 with the best fit line and the error envelope at 1σ of the fitted line. Fig. 2b shows the complementary projection along the plane onto the $\ln(K/Na)^{crd}$ vs $\sqrt{aH_2O}$ plane at 900 °C.

Thus from (17) the provisional thermometer is

$$T = -10890(\pm 3400) \Big/ \left[\ln\left(\frac{K}{Na}\right) - 9.539(\pm 2.850) + 1.303(\pm 0.427)\sqrt{aH_2O} \right] \quad (18)$$

where K and Na are in atoms per formula unit of cordierite and T is in Kelvin. This thermometer is only strictly valid for a melt with a $(Na/K)^{melt} = 1.39$. The accuracy but not the precision of the thermometer will decrease as the alkali ratio of the melt deviates from this value. The effect of the variation in melt composition is discussed in the section on limitations of this thermometer below.

Fig. 3 shows the predicted temperature for each of our original data points calculated from equation (18). The solid line is the predicted temperature for any nominal temperature in the experimental range. The dot-dash line drawn in this figure shows the 67.5% (*i.e.* 1σ) confidence envelope in fitting the line at a water activity of 0.5. It is effectively the precision of the calibration of the thermometer (Hodges & McKenna, 1987) and is unrealistically small when compared with the spread of the original data. This confidence envelope cannot be used as a prediction error, *i.e.* it does not give the accuracy of the thermometer. Errors in the predicted temperature based upon this regression equation will be significantly larger. The York fitting programme does not permit predicted errors to be determined from a previous calibration such as we need to do here. Hodges and McKenna (1987) describe a method of calculating realistic error in the accuracy of a thermometer by using a Monte Carlo approach for fitting a line in two dimensions. For three dimensions the problem becomes significantly more difficult. As a first and minimum approximation we have drawn in the dashed lines that include approximately 67% of the original data points (Fig. 3) and are thus 1σ uncertainties. Thus, for a water activity of 0.5, a predicted temperature of 900 °C has a 1σ error of approximately ±45 °C that is 5 times larger

than the error in fitting the plane (±9 °C 1σ) at these conditions. The prediction errors may appear large in comparison to the experimental range studied, however, this uncertainty compares favourably with other geothermometers [*e.g.* ±50 °C for garnet-biotite Fe-Mg exchange (Ferry & Spear, 1978); ±40 °C for garnet-orthopyroxene Fe-Mg exchange (Harley, 1984)]. When using this thermometer additional errors will result from any inhomogeneity in the cordierites analysed. However, when calculating temperature *differences* between cordierites for the same melt composition, these problems in determining the accuracy of the thermometer are not important and the more easily determined errors in the precision (see appendix) are all that is required.

Limitations of the thermometer

For the effectiveness of the provisional thermometer to be maximised there must be a granitic melt of close to a eutectic composition with a $(Na/K)^{melt}$ ratio of 1.39 in equilibrium with the cordierite. The proportion of melt must be large enough for the exchange of Na and K with the cordierite to not significantly affect the composition of the melt. We have not measured the effect of changing the melt composition in these experiments. However, we can estimate the range of compositions to which we can apply this thermometer by substituting different melt compositions into the equation and examining the deviation in the predicted temperature. The greatest contribution to the deviation in temperature is derived from the $\ln(Na/K)^{melt}$ term (= ln1.39) in parameter A of equation (16) but there is a small effect from the $(X^{melt}_{Na} - X^{melt}_{K})$ term (= 0.04) of the B parameter. If we take our previous assumption that the interaction parameter W_{KNa} must be less than 22 kJmol^{-1} (given the lack of unmixing in the melt at T ≤ 1300K) we can show that the thermometer is accurate within 20 °C if the melt composition is approximately $1.65 \leq \ln(Na/K)^{melt} \leq 1.19$ and $0.015 \leq (X^{melt}_{Na} - X^{melt}_{K}) \leq 0.085$. This defines a zone on a ternary Qz-Ab-Or plot that is roughly parallel to a line radial from the Qz apex. If we compare this to the range of experimentally determined eutectic minimum melt compositions illustrated in Figure 2.20 of Johannes & Holtz (1996) it is apparent that this range includes all minimum melt compositions at $aH_2O \leq 0.5$ for all pressures between 1 and 8 kbar. At higher water activities the eutectic melt compositions determined at higher pressures (*e.g.* over 2 kbar) will result in a larger temperature deviation. Given the limitations in the available experimental data and constraints on the value of the W_{KNa} interaction parameter, it is not possible to extend the thermometer presented above to these high pressure-high aH_2O conditions. At higher temperatures the thermometer may be applicable until cordierite melts, but it must be recognised that at such high temperatures there will also be more scope for variation in the composition of the melt and thus a greater likelihood of the thermometer giving inaccurate results.

Application of the thermometer to natural rocks is further complicated by the general inability to confidently estimate the composition of the last melt in equilibrium with cordierite from whole-rock chemical data. In plutonic rocks and migmatite leucosomes it is widely recognised that the measured rock compositions do not correspond to those of the minimum because of the effects of accumulation of early-formed minerals, restite and late-stage melt loss (*e.g.* Kriegsman, 2001; Sawyer, 1996). Hence, the best procedure for estimation of the appropriate minimum melt composition would be to use a diagram such as Figure 2.20 of Johannes & Holtz (1996) coupled with independent pressure and water activity (which can be established from the cordierite volatile content) estimates.

It is likely that the temperature determined by this thermometer would be that at which the cordierite was last in equilibrium with the melt, and thus the thermometer is most likely to give the temperature at which the melt crystallised or escaped. This assumes that there is no potential for change in cordierite K/Na subsequent to melt removal or crystallisation. However, if other K-Na bearing mineral phases such as micas or alkali feldspars are present following melt removal or crystallisation then the K/Na of cordierite may change through continued re-equilibration and exchange with these minerals. Clearly, in such cases the final K/Na measured in cordierite may bear no resemblance to that attained when cordierite and melt were in equilibrium.

Further important limitations on the use of this thermometer are imposed by the analytical precision of the electron microprobe. At low temperatures, of less than about 750 °C, K_2O will be very small and difficult to measure precisely as the detection limits of potassium on the electron probe are approximately 0.04 wt% K_2O. Also at the lower temperature end of the range the K/Na ratio will become very small *e.g.* at 700 °C and unit aH_2O the model K/Na ratio is only 0.05. This means that the relative errors in K/Na become larger, compounding the uncertainties arising from the detection limitations. This thermometer has only been calibrated with a Li- and Be-poor cordierite, and as a consequence the effects of these other components in the system are also unknown.

Comparison with previous studies on Na in cordierite

Knop & Mirwald (2000) describe a decrease in Na content of cordierite with temperature above the eutectic in the cordierite-albite system. The dashed line drawn in Fig. 1e shows the decrease in Na_2O with temperature observed by Knop & Mirwald (pers. comm.). The variation in the Na_2O with temperature that we observed is approximately an order of magnitude smaller than their results. In contrast to the results of Knop & Mirwald (2000), adding CO_2 to the system does not reduce the Na content, and the H_2O-undersaturated experiments and H_2O-CO_2 experiments are indistinguishable in Na_2O and K_2O. In addition, for the H_2O-CO_2 experiments there is no obvious systematic variation in Na_2O as the CO_2 content of the cordierite increases. The reason for this discrepancy between our data and that of Knop & Mirwald (2000) is not clear. Mirwald (1986) also identified a strong temperature effect on the sodium content in his experiments conducted on Mg-cordierite with NaOH at temperatures below the melting interval. His experiments at 800 °C contained similar quantities of sodium to ours but

the gradient was similar to Knop & Mirwald (pers. comm.). Knop & Mirwald (pers. comm.) also reported similar Na_2O *vs* T gradients in the cordierite-albite system below the eutectic but offset to lower sodium contents from the line shown in Fig. 1. They suggest that the gradient decreases, producing lower sodium contents, as the water activity is reduced. This would agree with our observation of there being a positive correlation between Na and H_2O, but the effect they observed was much greater than that which we tentatively identified from Fig. 1a and c.

The more interesting result of our work is the greater variation of potassium with both H_2O and temperature. Previous studies do not report such correlations and indeed the natural high-potassic cordierites of Schreyer *et al.* (1990) showed high electron microprobe totals that suggested cordierites were volatile-free. Although many papers ignore the potassium contents of cordierites by attributing them to the effects of pinitisation it is odd that the majority of relevant publications that do report potassium contents do not find such high levels as we have obtained in this experimental study. Our model is a simple one by comparison with natural rocks and there are clearly many other factors yet to be accounted for that may influence the system. For example, Na-K exchange between cordierite and other minerals such as biotite, muscovite and feldspar may reset the alkali contents during cooling at temperatures below those at which melt remains stable.

Our analytical method does not allow the two room temperature types of H_2O channel sites to be distinguished (Aines & Rossman, 1984). If the relationships of Visser *et al.* (1994) and Stolpovskya *et al.* (1998) were true for our experimental cordierites, the low Na and K contents in all samples would imply that the majority of the H_2O would lie in Type-I sites with the H-H vector lying parallel to the *c*-axis. Given the lack of a large variation in Na and K this would also imply that the Type-I site must accommodate the major changes in the H_2O content in these experimental cordierites. At experimental P-T conditions these sites for the H_2O may breakdown into a more disordered "free state" (Aines & Rossman, 1984). It is possible that other channel constituents may show similar behaviour at experimental conditions.

Conclusions

Our data has shown that there can be significant variations in the potassium content of cordierites in contact with a granitic melt of essentially fixed composition. The potassium compositions appear to be controlled in particular by temperature and water content, whereas sodium contents are near-constant. We have constructed a provisional thermometer based on these compositional features which may be useful for high-temperature, migmatitic cordierite-bearing rocks and should be tested further using high-quality data from such rocks. We recommend that sodium and potassium should be measured more frequently and carefully in natural cordierites as, with an estimate of the water activity, they may provide further clues to the crustal and metamorphic histories of high-grade terrains.

Acknowledgements: This research was funded by NERC grants GR3/9099 and GR3/12573 to SLH and PT. Robert Brown provided assistance with the experimental apparatus, Paula McDade with EMP analyses and John Craven with the SIMS analyses. PT's understanding of statistics was greatly improved by lengthy discussions with Julie Hollis, John Craven, Roy Thompson and Ian Main. Angelika Kalt, Peter Mirwald and Werner Schreyer provided detailed and constructive reviews for which we are extremely grateful.

References

Aines, R.D. & Rossman, G.R. (1984): The high temperature behaviour of water and carbon dioxide in cordierite and beryl. *Am. Mineral.,* **69**, 319-327.

Armbruster, T. (1986): Role of Na in the structure of low-cordierite: A single-crystal X-ray study. *Am. Mineral.,* **71**, 746-757.

Behrens, H. (1995): Determination of water solubility in high-viscosity melts: An experimental study on $NaAlSi_3O_8$ and $KAlSi_3O_8$ melts. *Eur. J. Mineral.,* **7**, 905-920.

Burnham, C.W. & Nekvasil, H. (1986): Equilibrium properties of granitic pegmatite magmas. *Am. Mineral.,* **71**, 239-263.

Carrington, D.P. & Harley, S.L. (1995): Partial melting and phase relations in high-grade metapelites: an experimental petrogenetic grid in the KFMASH system. *Contrib. Mineral. Petrol.*, **120**, 270-291.

–, – (1996): Cordierite as a monitor of fluid and melt water contents in the lower crust: and experimental calibration. *Geology*, **24**, 647-650.

Clemens, J.D. & Wall, V. (1984): Origin and evolution of a peraluminous silicic ignimbrite suite – the Violet Town volcanics. *Contrib. Mineral. Petrol.,* **88**, 354-371.

Ferry, J.M. & Spear, F.S. (1978): Experimental calibration of the partitioning of Fe and Mg between biotite and garnet. *Contrib. Mineral. Petrol.*, **66**, 113-117.

Fitzsimons, I.C.W. (1996): Metapelitic migmatites from Brattstrand Bluffs, east Antarctica – metamorphism, melting and exhumation of the mid-crust. *J. Petrol.,* **37**, 395-414.

Flood, R.H. & Shaw, S.E. (1975): A cordierite bearing Granite Suite from the New England Batholith, N.S.W, Australia. *Contrib. Mineral. Petrol.,* **52**, 157-164.

Harley, S.L. (1984): An experimental study of the partitioning of Fe and Mg between garnet and orthopyroxene. *Contrib. Mineral.* Petrol., **86**, 359-373.

Harley, S.L. & Carrington, D.P. (2001): The distribution of H_2O between cordierite and granitic melt: Improved calibration of H_2O incorporation in cordierite and its application to high-grade metamorphism and crustal anatexis. *J. Petrol.*, **42**, 1595-1620.

Harley, S.L., Thompson, P., Buick, I.S., Hensen, B.J. (2001): Cordierite as a sensor of high-grade metamorphic processes. *J. Metam. Geol.,* **20**, 71-86.

Hodges, K.V. & McKenna, L.W. (1987): Realistic propagation of uncertainties in geologic thermobarometry. *Am. Mineral.*, **72**, 671-680.

Holland, T.J.B. & Powell, R. (1998): An internally consistent thermodynamic data set for phases of petrologic interest. *J. Metam. Geol.*, **16**, 309-343.

Johannes, W. & Holtz, F. (1996): Petrogenesis and experimental petrology of granitic rocks. Springer Verlag, Berlin, 346 p.

Johannes, W. & Schreyer, W. (1981): Experimental introduction of CO_2 and H_2O into Mg-cordierite. *Am. J. Sci.*, **281**, 299-317.

Kalt, A., Altherr, R., Ludwig, T. (1998): Contact Metamorphism in pelitic rocks on the island of Kos (Greece, Eastern Aegean Sea): a test for the Na-in-cordierite thermometer. *J. Petrol.,* **39**, 663-668.

Kim, Y.H., Mercurio, D., Mercurio, J.P., Fritt, B. (1984): Structural study of a K-substituted synthetic cordierite. *Mat. Res. Bull.*, **19**, 209-217.

Knop, E. & Mirwald, P.W. (2000): Cordierite as a monitor of fluid and melt sodium activity in metapelites, migmatites and granites: constraints from incorporation experiments. Experimental Mineralogy Petrology and Geochemistry VIII, Bergamo, Italy. *J. Conf. Abstracts,* **5**, 58.

Kolesov, B.A. & Geiger, C.A. (2000): Cordierite II: The role of CO_2 and H_2O. *Am. Mineral.,* **85**, 1265-1274.

Kriegsman, L.M. (2001): Partial melting, partial melt extraction and partial back reaction in anatectic migmatites. *Lithos*, **56**, 75-96.

Ludwig, K.R. (1992): ISOPLOT Version 2.92. Unpublished computer program. Berkley Geochronology Center, University of California.

Minitab 12: http://www.minitab.com, Minitab Inc., 3081 Enterprise Drive, State College PA 16801-3008 USA.

Mirwald, P.W. (1986): Ist cordierite ein geothermometer? *Fortschr. Mineralogie,* **64**, Beih. 1, 119.

Sawyer, E.W. (1996): Melt segregation and magma flow in migmatites: Implications for the generation of granite magmas. *Trans. Roy. Soc. Edin. – Earth Sciences*, **87**, 85-94.

Schreyer, W. (1985): Experimental studies on cation substitutions and fluid incorporation in cordierite. *Bull. Mineral.,* **108**, 273-291.

Schreyer, W., Gordillo, C.E., Werding, G. (1979): A new sodian-beryllian cordierite from Soto, Argentina and the relationship between distortion index, Be content and state of hydration. *Contrib. Mineral. Petrol.,* **70**, 421-428.

Schreyer, W., Maresch, W.V., Daniels, P., Wolfsdorff, P. (1990): Potassic cordierites: Characteristic minerals for high-temperature, very low-pressure environments. *Contrib. Mineral. Petrol.,* **105**, 162-172.

Spear, F. (1993): Metamorphic phase equilibria and pressure-temperature-time paths. Mineralogical Society of America Monograph., Bookcrafters Inc., Michigan.

Stolpovskya, V.N., Sokol, E.V., Lepezin, G.G. (1998): IR spectroscopy of water in cordierites. *Geologiya i Geofizika,* **39**, 65-73.

Thompson, P., Harley, S.L., Carrington, D.P. (2001): H_2O-CO_2 partitioning between fluid, cordierite and granitic melt at 5 kbar and 900 °C. *Contrib. Mineral. Petrol.,* **142**, 107-118.

Visser, D., Kloprogge, J.T., Maijer, C. (1994): An infrared spectroscopic (IR) and light-element (Li, Be, Na) study of cordierites from the Bamble sector, South Norway. *Lithos,* **32**, 95-107.

Wood, B.J. & Fraser, D.G. (1977): Elementary thermodynamics for geologists. Oxford University Press.

Wolfsdorff, P. & Schreyer, W. (1992): Synthesis of sodian cordierites in the system Na_2O-MgO-Al_2O_3-SiO_2. *Neues Jb. Mineral.* Mh., **1992**, 80-96.

York, D. (1967): The best isochron. *Earth Planet. Sci. Lett.*, **2**, 479-482.

– (1969): Least squares fitting of a straight line with correlated errors *Earth Planet. Sci. Lett.*, **5**, 320-324.

Received 18 January 2001
Modified version received 24 July 2001
Accepted 5 November 2001

Appendix on error propagation methods

The general formula used for error propagation is

$$\sigma_y^2 = \sum_{i=1}^{n}\sum_{j=1}^{n}\left(\frac{\delta y}{\delta x_i}\right)\left(\frac{\delta y}{\delta x_j}\right)\sigma_{x_i}\sigma_{x_j}\rho_{x_i x_j}\,. \tag{A1}$$

Thus, for calculating the plane fitting errors in T from the errors in A, B and C, the ternary expansion of (A1) will be

$$\begin{aligned}\sigma_T^2 \approx{}& \left(\frac{\delta T}{\delta A}\right)_{BC}^2\sigma_A^2 + \left(\frac{\delta T}{\delta B}\right)_{AC}^2\sigma_B^2 + \left(\frac{\delta T}{\delta C}\right)_{AB}^2\sigma_C^2 \\ &+ 2\left\{\rho_{AB}\sigma_A\sigma_B\left(\frac{\delta T}{\delta A}\right)\left(\frac{\delta T}{\delta B}\right) + \rho_{BC}\sigma_B\sigma_C\left(\frac{\delta T}{\delta B}\right)\left(\frac{\delta T}{\delta C}\right)\right. \\ &\left. + \rho_{AC}\sigma_A\sigma_C\left(\frac{\delta T}{\delta A}\right)\left(\frac{\delta T}{\delta C}\right)\right\},\end{aligned} \tag{A2}$$

where for equation (15)

$$\left(\frac{\delta T}{\delta A}\right) = B\Big/\left[\ln\left(\frac{K}{Na}\right)^{crd} - A - C\sqrt{aH_2O}\right]^2, \tag{A3}$$

$$\left(\frac{\delta T}{\delta B}\right) = 1\Big/\left[\ln\left(\frac{K}{Na}\right)^{crd} - A - C\sqrt{aH_2O}\right], \tag{A4}$$

$$\left(\frac{\delta T}{\delta C}\right) = B\sqrt{aH_2O}\Big/\left[\ln\left(\frac{K}{Na}\right)^{crd} - A - C\sqrt{aH_2O}\right]^2 \tag{A5}$$

and the values of σ_A, σ_B, σ_C, ρ_{AB}, ρ_{BC} and ρ_{AC} can be found from Table 3.